Vol 13 No 4, April 2004
1009-1963/2004/13(04)/0516-06

Chinese Physics

© 2004 Chin. Phys. Soc.
and IOP Publishing Ltd

Effect of phonon scattering mechanisms on the lattice thermal conductivity of skutterudite-related compound*

Yang Lei(杨 磊), Wu Jian-Sheng(吴建生), and Zhang Lan-Ting(张澜庭)†

Key Laboratory of the Ministry of Education for High Temperature Materials and Testing, School of Materials Science and Engineering, Shanghai Jiaotong University, Shanghai 200030, *China*

(Received 28 July 2003; revised manuscript received 4 November 2003)

We have prepared the skutterudite-related compounds $FeCo_3Sb_{12}$ and $La_{0.75}Fe_3CoSb_{12}$ with different average grain sizes (about 0.8 and 3.9μm) by hot pressing. Samples were characterized by XRD, EPMA and SEM. The lattice thermal conductivity was investigated in the temperature range from room temperature to 200°C. Based on the Debye model, we analyse the change in lattice thermal conductivity due to various phonon scattering mechanisms by examining the relationship between the weighted phonon relaxation time $\tau(\omega/\omega_D)^2$ and the reduced phonon frequency ω/ω_D. The effect of grain boundary scattering to phonon is negligible within the range of grain sizes considered in this study. The large reduction in lattice thermal conductivity of $FeCo_3Sb_{12}$ compound contributes to the electron–phonon scattering. As for $La_{0.75}Fe_3CoSb_{12}$ compound, the atoms of La filled into the large voids in the structure of the skutterudite produce more significant electron–phonon scattering as well as more substitute of Fe at Co site at the same time. Moreover, the point-defect scattering appears due to the difference between the atoms of La and the void. In addition, the scattering by the rattling of the rare-earth atoms in the void is another major contribution to the reduced lattice thermal conductivity. Introducing the coupling of the electron–phonon scattering with the point-defect scattering and the scattering by the rattling of the rare-earth atom is an effective method to reduce the lattice thermal conductivity of the skutterudite-related compounds by substitution of Fe for Co and the atoms of La filled in the large voids in the skutterudite structure.

Keywords: skutterudite-related compound, lattice thermal conductivity, phonon scattering mechanism

PACC: 7215, 6166, 6320

1. Introduction

Skutterudite compounds MX_3 with the cubic structure (M=Co, Rh, Ir, Fe, Ru, X=P, As, Sb.) have been shown to possess good thermoelectric properties [1–4] and have received considerable attention over the past several years because of their potential as a prospective material for applications in thermoelectric generators and refrigerators. Although binary skutterudite compounds have good electrical transport properties, their overall ZT (figure of merit) is not high due to the relatively high thermal conductivity. Doping [5–7] and alloying [8,9] are very effective at reducing the thermal conductivity of this compound. It is found by Sales *et al* [10–13] that rare-earth atoms such as La, Ce, etc may be inserted into the voids of the crystal structure where they 'rattle' around their equilibrium positions. This rattling motion can efficiently scatter phonons and thus greatly reduce the lattice thermal conductivity without deteriorating the electrical transport properties. Filled skutterudite materials have ZT values as high as 1.0 within the temperature range from room temperature to 700°C and are one family of materials possessing the highest values of ZT.[14–16]

In order to investigate the essential mechanism of the reduction in thermal conductivity of the skutterudite-related compound and find what kinds of phonon scattering mechanisms play an important role in reducing the lattice thermal conductivity of the skutterudite-related compound, we have prepared the skutterudite-related compound $FeCo_3Sb_{12}$ and $La_{0.75}Fe_3CoSb_{12}$ with different average grain sizes

*Project supported by the National Natural Science Foundation of China (Grant No 59902003).
†E-mail: lantingzh@sjtu.edu.cn

(about 0.8 and 3.9μm) by hot pressing and investigated the change of the lattice thermal conductivity. The phonon transport properties are compared with the theoretical calculations based on the Debye model, which was applied to $Si_{1-x}Ge_x$ by Steigmeier and Abeles,[17] in order to obtain detailed information about the phonon scattering mechanism in the skutterudite-related compound.

2. Experimental procedures

High purity La shot (99.9%), Sb shot (99.998%), Fe rod (99.9%), and Co shot (99.9%) were used as the starting materials to prepare samples with two different compositions (Table 1). In order to avoid reaction between the rare-earth element and quartz tube, a thin layer of carbon was deposited on the inside of a round-bottomed quartz tube by the pyrolysis of acetone. Then stoichiometric amounts of these materials were loaded into the precarbonized quartz tube. The quartz tube was sealed under vacuum at a pressure of 10^{-3} Pa and 2×10^4 Pa of ultrahigh purity argon, and heated in a muffle furnace. The quartz tube was heated to 600°C at a rate of 2°C/min, kept at 600°C for 3h, slowly (1°C/min) heated to 1100°C and kept for 24h, and then cooled to 1000°C and kept for 24h and quenched into water. It was necessary to heat the quartz tube slowly because of the highly exothermic reaction between the rare-earth elements and Sb. After quenching, the same quartz tube (containing the pretreated ingot) was annealed at 700°C for 100h to form the exact skutterudite phase. In order to form a completely dense polycrystalline ingot, the reacted material was ground with agate mortar, and then was milled into different sized powders with a planetary attrition mill. The attrition mill was composed of agate ball, a stainless steel central shaft with arms and an agate container. The milled powders were loaded into a graphite die for hot pressing. Hot pressing was conducted under a pressure of 60MPa. All samples were heated at a rate of 30°C/min and hot pressed for 1–2h under vacuum at 600–650°C.

The phase constitutions of the samples were determined by powder x-ray diffraction (Rigaku: RAD–C, Cu$K\alpha$). Chemical composition of the skutterudite phase and microstructure of samples were determined using electron probe microanalyser (EPMA). The fracture surfaces of samples were investigated using scanning electron microscope (SEM), and the transversal method was used to determine the average grain size of the samples. Measurements of the Hall coefficient R_H and the electrical resistivity were carried out in a temperature range from room temperature to 500°C using the van der Pauw technique in an argon atmosphere. The Hall carrier concentration n was determined from the Hall coefficient R_H using $n = 1/R_H e$ relation, where e is the electron charge. The measurement of Seebeck coefficient was performed by applying a small temperature difference (3°C) to the two ends of a specimen in a temperature range from room temperature to 500°C in an argon atmosphere. The specific heat capacity was measured by DSC in Ar flow. The thermal diffusivity was measured by the AC calorimetry method in a temperature range from room temperature to 200°C. The thermal conductivity was calculated from the experimental values of thermal diffusivity, specific heat capacity and density. Densities of samples were determined by the Archimedes method.

3. Results and discussion

Figure 1 displays typical x-ray diffraction (XRD) patterns of $FeCo_3Sb_{12}$ and $La_{0.75}Fe_3CoSb_{12}$ samples after hot pressing. All the samples display peaks characteristic of the skutterudite structure, from which lattice constants can be determined. The lattice constants of $FeCo_3Sb_{12}$ and $La_{0.75}Fe_3CoSb_{12}$ samples are 0.906 and 0.910nm, respectively. The lattice parameters of these samples are larger than that of binary $CoSb_3$ (0.9032nm[13]) due largely to Fe substitution for Co and the atoms of La filled into the large void in the structure of the skutterudite compound. For $FeCo_3Sb_{12}$, a slight amount of Sb and $FeSb_2$ was identified by XRD, which was also found in EPMA observations. The results of EPMA show that all the samples are homogeneous and their compositions are

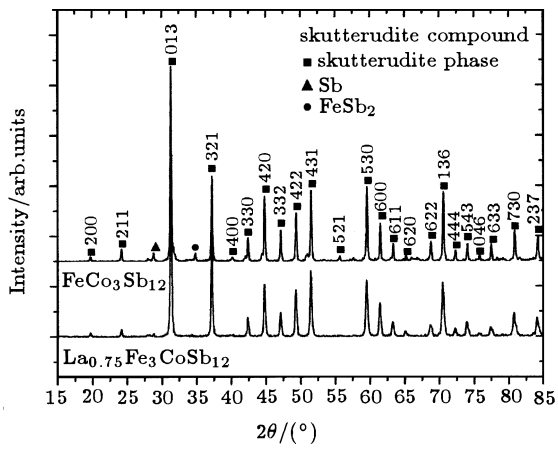


Fig.1. XRD patterns of $FeCo_3Sb_{12}$ and $La_{0.75}Fe_3CoSb_{12}$ samples.

very close to the nominal ones. Average grain sizes of the samples are listed in Table 1. Typical fractured surfaces of $FeCo_3Sb_{12}$ having different grain sizes of about 0.8 and 3.9μm are shown in Fig.2. The densities of the samples were determined to be more than 90% the theoretical values by using the Archimedes method.

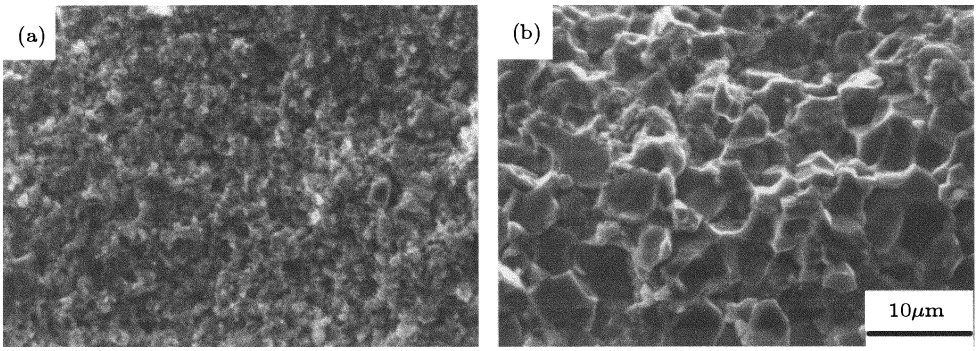


Fig.2. Typical fractured surfaces of $FeCo_3Sb_{12}$ after hot pressing, showing different grain sizes (a) 0.8μm and (b) 3.9μm.

Table 1. The grain size, Seebeck coefficient, carrier concentration and mobility for $FeCo_3Sb_{12}$ and $La_{0.75}Fe_3CoSb_{12}$ compounds at room temperature.

No	Sample	Grain size/μm	Seebeck coefficient/(μVK^{-1})	Carrier concentration/cm^{-3}	Mobility/(cm^{2}V^{-1}S^{-1})
1#	($FeCo_3Sb_{12}$)	0.8	51	1.3×10^{20}	61
2#	($FeCo_3Sb_{12}$)	3.9	49	1.9×10^{20}	36
3#	($La_{0.75}Fe_3CoSb_{12}$)	0.8	70	3.0×10^{20}	16
4#	($La_{0.75}Fe_3CoSb_{12}$)	3.9	93	5.0×10^{20}	10

Table 1 lists the samples prepared in this study, their grain sizes, Seebeck coefficients, carrier concentrations, and mobilities measured at room temperature. The thermal conductivity in the temperature range from room temperature to 200°C was measured for all the samples. The thermal conductivity can be represented by the sum of an electronic component and a lattice component as $\kappa = \kappa_e + \kappa_g$; the electronic component can be calculated according to the Wiedemann–Franz law: $\kappa_e = L\sigma T$, where L is the Lorenz number, σ is the electrical conductivity, and T is the absolute temperature. Assuming the Lorenz number L to be $L = 2.0 \times 10^{-8}\mathrm{V}^2\mathrm{K}^{-2}$,[13] the electronic thermal conductivity κ_e is obtained, and the lattice thermal conductivity κ_g can be estimated by subtracting the electronic contribution from κ. In the case of a slight amount of porous in the samples, the values of the lattice thermal conductivity should be corrected for porosity.[18,19] Figure 3 shows the temperature dependence of the lattice thermal conductivity for all the samples with different grain sizes, compared with that of binary $CoSb_3$.[20] From Fig.3, the lattice thermal conductivity of all the samples is much smaller than that of $CoSb_3$. The substitution of Fe for Co causes additional decrease in lattice thermal conductivity, but its origin has not been determined.[21,22] Additionally, in $La_{0.75}Fe_3CoSb_{12}$ samples, we can see further decrease in lattice thermal conductivity relative to $FeCo_3Sb_{12}$ samples. One reason for this is attributed to high amount of Fe substitution at Co site, and another reason is that the atoms of La fill in the large voids in the structure of the skutterudite

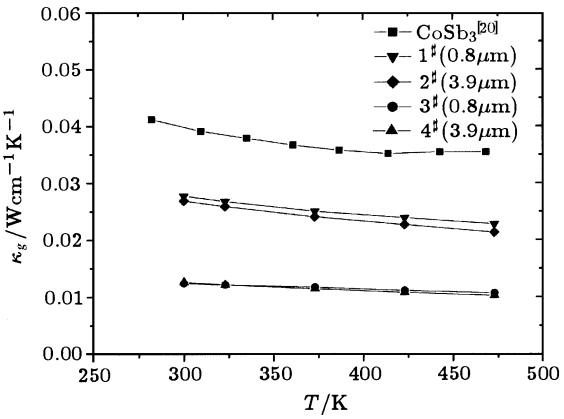


Fig.3. Temperature dependence of the lattice thermal conductivity for $FeCo_3Sb_{12}$ and $La_{0.75}Fe_3CoSb_{12}$ compounds with different grain sizes, compared with that of $CoSb_3$.[20]

compounds and 'rattle' in these voids, thus enhancing the scattering of phonons. From the results of thermal conductivity, it is concluded that the lattice thermal conductivity of these samples is almost independent of the grain size, within the range of grain sizes considered in this study.

In order to discuss the scattering mechanisms of phonons in the skutterudite-related compounds $FeCo_3Sb_{12}$ and $La_{0.75}Fe_3CoSb_{12}$, we performed theoretical calculations of the lattice thermal conductivity using a theory of relaxation time of phonons based on the Debye model,[23]

$$k_g = \frac{k_B}{2\pi^2 v}\left(\frac{k_B}{\hbar}\right)^3 \int_0^{\theta/T} \tau \frac{x^4 e^x}{(e^x-1)^2} dx, \qquad (1)$$

where $x = \hbar\omega/k_B T$, ω is the phonon frequency, k_B is the Boltzmann constant, $\hbar = h/(2\pi)$, h is Planck's constant, T is the absolute temperature, the sound velocity v from Ref.[5] is $4.59 \times 10^3 ms^{-1}$, and τ is the phonon relaxation time. The model calculation takes into account (a) three-phonon scattering, including normal (N) and umklapp (U) processes, (b) point-defect (alloy) scattering, (c) electron–phonon scattering. In order to compare with the experimental result of the lattice thermal conductivity, we introduce the grain boundary scattering. In the absence of calculative model about scattering of the rattling of rare-earth atoms in the voids, the relaxation time of phonons due to this mechanism was not calculated for $La_{0.75}Fe_3CoSb_{12}$ compound. Therefore, the total relaxation time of phonons τ can be given by

$$\tau^{-1} = \tau_N^{-1} + \tau_U^{-1} + \tau_{PD}^{-1} + \tau_{EP}^{-1} + \tau_B^{-1}, \qquad (2)$$

where τ_N, τ_U, τ_{PD}, τ_{EP}, and τ_B are relaxation times for N, U, point-defect, electron–phonon, and grain boundary scatterings.

Assuming that the lattice thermal conductivity of undoped $CoSb_3$ is dominated by normal (N) and umklapp (U) processes, τ_U can be given by [15]

$$\tau_U^{-1} = \frac{1}{b_0}\frac{\pi}{4}\left(\frac{k_B}{2\pi^2 v}\right)\frac{k_B^3 T^3}{\hbar^3\theta^2}\frac{n^{2/3}\gamma^2}{M\delta}x^2, \qquad (3)$$

where b_0 is a constant equal to $3.04 \times 1^7 s^{-3}K^{-3}$,[23] θ is the Debye temperature (θ=307K for skutterudite compound [23]), M is the total average mass for $CoSb_3$, γ is the Grüneisen constant, assumed to be 1.23,[23] and δ is the atomic size determined by the cubic root of the atomic volume, for skutterudite lattice $\delta = (a^3/32)^{1/3}$.[7] This is similar to the form of τ_U used by White and Klemens [24] and Vining [25] for Si–Ge systems, but includes the crystal complexity factor $n^{2/3}$.[23] τ_N can be given by [17]

$$\tau_N^{-1} = \beta\tau_U^{-1}, \qquad (4)$$

where β is the ratio of N to U, and is assumed to be temperature-independent; we assume the value of β to be 2.75 for the skutterudite compound.[13]

First, we consider the point defect as a source of extrinsic scattering in our compounds. The relaxation time τ_{PD} is given by [17]

$$\tau_{PD}^{-1} = (\delta^3\Gamma/4\pi v^3)\omega^4, \qquad (5)$$

where Γ is the scattering parameter. For impurity atoms on a single atomic site $\Gamma = \sum f_i(1-M_i/M_{av})^2$, where $M_{av} = \sum f_i M_i$. Here, f_i is the fractional concentration of impurity atom i, and M_i is its mass. In principle, one should also include the influence of strain, but since the lattice constants of $FeCo_3Sb_{12}$ and $La_{0.75}Fe_3CoSb_{12}$ compounds and undoped $CoSb_3$ differ by only about 1%, the effect will be small compared with the mass fluctuation. For a single type of impurity atom with relative concentration α, the scattering parameter reduces to $\Gamma = \alpha(1-\alpha)(\Delta M/M_{av})^2$, where ΔM is the difference between the mass of the impurity and that of the host. For a compound $U_uV_vW_w$, the composite scattering parameter Γ, denoted by $\Gamma(U_uV_vW_w)$, is given by [22]

$$\Gamma(U_uV_vW_w) = \frac{u}{u+v+w}\left(\frac{M_u}{M_m}\right)^2\Gamma(U) + \frac{v}{u+v+w}\left(\frac{M_v}{M_m}\right)^2\Gamma(V) + \frac{w}{u+v+w}\left(\frac{M_w}{M_m}\right)^2\Gamma(W), \qquad (6)$$

where $M_m = (uM_u + vM_v + wM_w)/(u+v+w)$.

Next, we consider the electron–phonon scattering. An estimate of the relaxation time τ_{EP} due to this process is given in Ref.[17] as (for $T = \theta$)

$$\tau_{EP}^{-1} = \frac{E_d^2 m^{*3} v}{4\pi\hbar^4 d}\left\{\frac{kT}{\frac{1}{2}m^* v^2}\right\}\left\{\frac{\hbar\omega}{kT} - \ln\frac{1+\exp\left[\left(\frac{1}{2}m^*v^2 - E_F\right)/kT + \hbar^2\omega^2/8m^*v^2kT + \hbar\omega/2kT\right]}{1+\exp\left[\left(\frac{1}{2}m^*v^2 - E_F\right)/kT + \hbar^2\omega^2/8m^*v^2kT - \hbar\omega/2kT\right]}\right\}, \qquad (7)$$

where E_d is the deformation potential, m^* is the density-of-states effective mass, d is the density, and E_F is the Fermi energy.

Finally, we consider the relaxation time due to the grain boundary scattering. The relaxation time τ_B is estimated as [24]

$$\tau_B^{-1} = \frac{v}{l}, \tag{8}$$

where l is the average grain size. We have determined the grain size in our samples to be 0.8 and 3.9μm.

We determined the values of the electron effective mass, the deformation potential, and the reduced Fermi energy based on the experimental data of Seebeck coefficient, carrier concentration, carrier mobility, density, and grain size (as shown in Table 1) using a single parabolic band model with acoustic phonon scattering which was found to be the predominant carrier scattering mechanism at around room temperature.[5] Details about the calculations of these parameters are presented in Refs.[5] and [7]. Then, we can obtain the total relaxation time τ based on Eqs.(2)–(8).

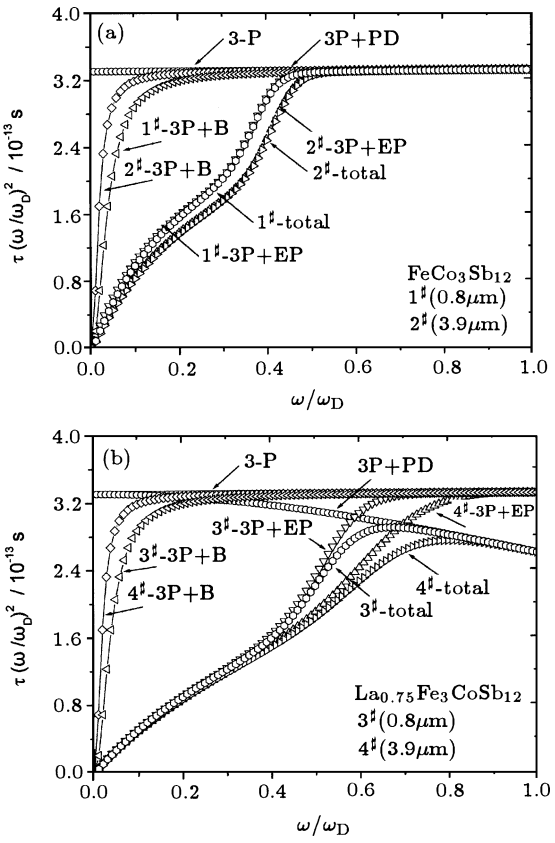


Fig.4. Weighted phonon relaxation time $\tau(\omega/\omega_D)^2$ as a function of reduced phonon frequency ω/ω_D for (a) $FeCo_3Sb_{12}$ and (b) $La_{0.75}Fe_3CoSb_{12}$, showing three-phonon scattering, point-defect scattering, electron–phonon scattering, grain boundary scattering, and their combinations.

In order to determine which phonon scattering mechanism contributes dominantly to the lattice thermal conductivity, it is useful to examine the relationship between the weighted phonon relaxation time $\tau(\omega/\omega_D)^2$ and the reduced phonon frequency ω/ω_D. This is plotted in Figs.4(a) and (b) for $FeCo_3Sb_{12}$ and $La_{0.75}Fe_3CoSb_{12}$ based on the calculated results of the total relaxation time, respectively. According to Eq.(1), the values of the lattice thermal conductivity are proportional to the areas under the curves. From Figs.4(a) and (b), the lattice thermal conductivities of the samples with different grain sizes are almost the same, and they are consistent with the experimental results. It is seen that the point-defect scattering cuts out the high-frequency phonons, while the electron–phonon scattering reduces the mean free path of the low-frequency phonons. However, since the estimated relaxation time of phonons for the grain boundary scattering is much larger than those for the scattering process considered, the effect of grain boundary scattering for phonons is negligible, as compared with other scattering processes. As for the $FeCo_3Sb_{12}$ compound, Fe and Co have only 3% mass difference, so the contribution of the point-defect scattering for the change of the lattice thermal conductivity is very small. So the large reduction in lattice thermal conductivity can be attributed mainly to the substitution of Fe for Co, resulting in the addition of electron–phonon scattering to the binary compound $CoSb_3$. For the $La_{0.75}Fe_3CoSb_{12}$ compound, the filling of La atoms into the large voids in the structure of the skutterudite compounds together with the replacement of Co by Fe lead to a larger electron–phonon scattering. Meanwhile, the point-defect scattering is produced to lead to additional decrease in lattice thermal conductivity due to the mass fluctuation between the La atoms filled and the large voids in the structure. The coupling of the electron–phonon scattering with the point-defect scattering leads to further decrease in lattice thermal conductivity for $La_{0.75}Fe_3CoSb_{12}$ compound. The model calculation basically explains the observed large reduction in the lattice thermal conductivity. For the La-filled skutterudite compounds, although the scattering mechanism of the rattling of rare-earth atoms around their equilibrium position is not included in the calculation, it is another major contribution to the reduction of lattice thermal conductivity. It is estimated that this accounts for perhaps 70% of the thermal resistivity.[26] This scattering mechanism of phonons

will cause more reduction in the lattice thermal conductivity of the $La_{0.75}Fe_3CoSb_{12}$ compound due to the coupling of the electron–phonon scattering with the point-defect scattering. Thus it is concluded that the larger reduction in the lattice thermal conductivity for the $La_{0.75}Fe_3CoSb_{12}$ compound can be attributed to the coupling of the electron–phonon scattering with the point-defect scattering and the scattering by the rare-earth atom 'rattling' in the voids. In this study, Fe is ferromagnetic, and the scattering from magnetic ion should play some role in the reduction of the lattice thermal conductivity. However, we have not considered the scattering from magnetic ions in this study. More experimental information about this aspect is necessary in order to carry out a more rigorous analysis.

4. Conclusions

We have prepared the skutterudite-related compounds $FeCo_3Sb_{12}$ and $La_{0.75}Fe_3CoSb_{12}$ with different grain sizes (0.8 and 3.9μm) and investigated the change of the lattice thermal conductivity. From our theoretical analysis based on the Deybe model, the grain boundary scattering is not significant, within the range of grain sizes considered in this study; substitution of Fe for Co causes additional reduction in lattice thermal conductivity due to producing a significant electron–phonon scattering in $FeCo_3Sb_{12}$ compound; the coupling of electron–phonon scattering with point-defect scattering leads to more decrease in lattice thermal conductivity for $La_{0.75}Fe_3CoSb_{12}$ compound due to the substitution of more Fe at the Co site and the filling of La atoms in the large voids in the skutterudite structure. In addition, the scattering of the rattling of the rare-earth atoms in the voids is another major contribution to the reduction of lattice thermal conductivity. It is concluded that the coupling of the electron–phonon scattering with the point-defect scattering and the scattering due to the rattling of the rare-earth atoms in the voids is an effective method to reduce the lattice thermal conductivity of the skutterudite-related compound by substituting Fe for Co and filling the La atoms in the large voids in the skutterudite structure. More information is needed, especially for the investigation of the possible magnetic ion scattering, for a more rigorous analysis.

References

[1] Morelli D T and Meisner G P 1997 *Phys. Rev.* B **56** 7376

[2] Morelli D T, Caillat T, Fleurial J P, Borshchevsky A, Vandersande J, Chen B and Uher C 1995 *Phys. Rev.* B **51** 9622

[3] Caillat T, Fleurial J P and Borshchevsky A 1996 *J. Crystal Growth* **166** 722

[4] Nolas G S, Slack G A, Caillat T and Meisner G P 1996 *J. Appl. Phys.* **79** 2622

[5] Caillat T, Borshchevsky A and Fleurial J P 1996 *J. Appl. Phys.* **80** 4442

[6] Matsubara K, Iyanaga T, Tsubouchi T, Kishimoto K and Koyanagi T 1994 in *Proc. 13*$^{\text{th}}$ *Int. Conf. on Thermoelectrics* p226

[7] Anno H, Matsubara K, Notohara Y, Sakakibara T and Tashiro H 1999 *J. Appl. Phys.* **86** 3780

[8] Caillat T, Kulleck J, Borshchevsky A and Fleurial J P 1996 *J. Appl. Phys.* **79** 1141

[9] Borshchevsky A, Caillat T and Koyanagi T 1996 in *Proc. 17*$^{\text{th}}$ *Int. Conf. on Thermoelectrics* p112

[10] Sales B C, Mandrus D and Williams R K 1996 *Science* **22** 1325

[11] Nolas G S, Slack G A, Morelli D T, Tritt T M and Ehrlich A C 1996 *J. Appl. Phys.* **79** 4002

[12] Sales B C, Mandrus D, Chakoumakos B C, Keppens V and Thompson J R 1997 *Phys. Rev.* B **56** 15081

[13] Nolas G S, Cohn J L and Slack G A 1998 *Phys. Rev.* B **58** 164

[14] Sales B C, Mandrus D and Williams R K 1996 *Science* **22** 1325

[15] Tang X F, Chen L D, Goto T, Hirai T and Yuan R Z 2000 *Acta Phys. Sin.* **49** 2196 (in Chinese)

[16] Tang X F, Chen L D, Goto T and Hirai T 2000 *Acta Phys. Sin.* **49** 2460 (in Chinese)

[17] Steigmeier E F and Abeles B 1964 *Phys. Rev.* **136** A1149

[18] Loeb S L 1954 *J. Am. Ceram. Soc.* **37** 96

[19] Francl J and Kingery W D 1954 *J. Am. Ceram. Soc.* **37** 99

[20] Fleurial J P, Caillat T and Borshchevsky A 1998 in *Proc. 16*$^{\text{th}}$ *Int. Conf. on Thermoelectrics* p914

[21] Chen B X, Xu J H, Uher C, Morelli D T, Merisner G P, Fleurial J P, Caillat T and Borshchevsky A 1997 *Phys. Rev.* B **55** 1476

[22] Meisner G P, Morelli D T, Hu S Q, Yang J H and Uher C 1998 *Phys. Rev. Lett.* **80** 3551

[23] Stokes K L, Ehrlich A C and Nolas G S 1999 *Mater. Res. Soc. Symp.* **545** 339

[24] White D P and Klemens P G 1992 *J. Appl. Phys.* **71** 4258

[25] Vining C B 1991 *J. Appl. Phys.* **69** 331

[26] Uher C 2001 *Semicond. Semimetals* **69** 238